

Supplementary Information

**Manganese-Cobalt Oxide as Effective Bifunctional Cathode for Rechargeable Zn-Air
Battery with a Compact Quad-Cell Battery Design**

Khaleel Ahmed J. Dilshad and M. K. Rabinal*

Dept. of Physics, Karnatak University, Dharwad – 580003, India

*Corresponding Author: mkrabinal@yahoo.com

Figure S1 (a)

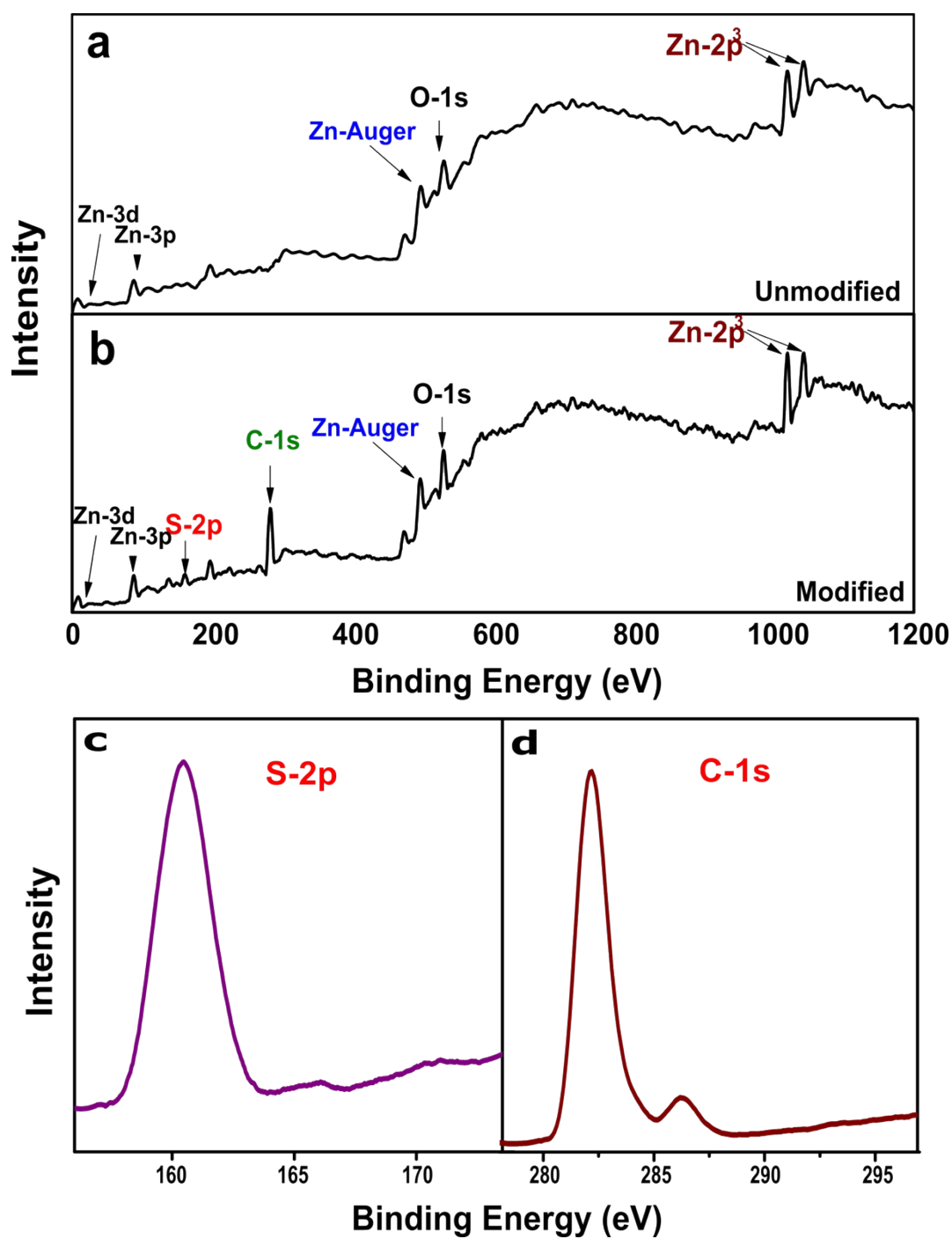


Figure S1a : Molecularly modified surface characterization results: **a)** full survey XPS spectrum of MPA treated Zn substrate prior to electrodeposition, **b)** unmodified zinc, **c)** and **d)** are high resolution XPS core spectra of S-2p and C-1s, respectively

Figure S1 (b)

FESEM images of unmodified and modified Zn are depicted in Figure S1. Clearly, the changes in surface structure of MPA-modified Zn can be observed compared to unmodified planar Zn.

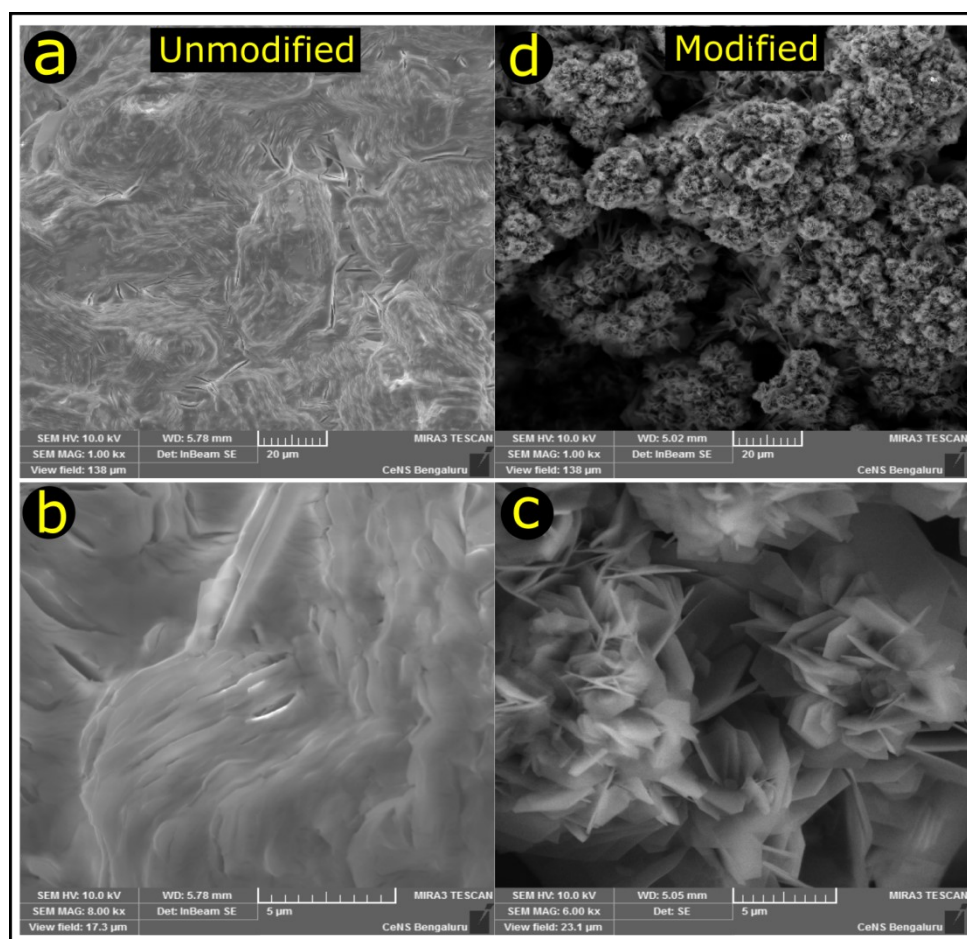


Figure S1b: FESEM images of electrodeposited zinc on unmodified Zn substrate [(a, b) low and high magnification, respectively], and modified Zn [(c, d) low and high magnification, respectively].

Figure S2

Electrochemical performance comparison data of Zn-Air battery assembled before and after zinc plate modification is shown below. The cycle stability of battery is examined by using a ‘test-cathode’. Clearly, the modified Zn outperforms the unmodified planar Zn anode which is the basis for using modified anode opposite to bimetallic oxide air cathode catalyst in the present study.

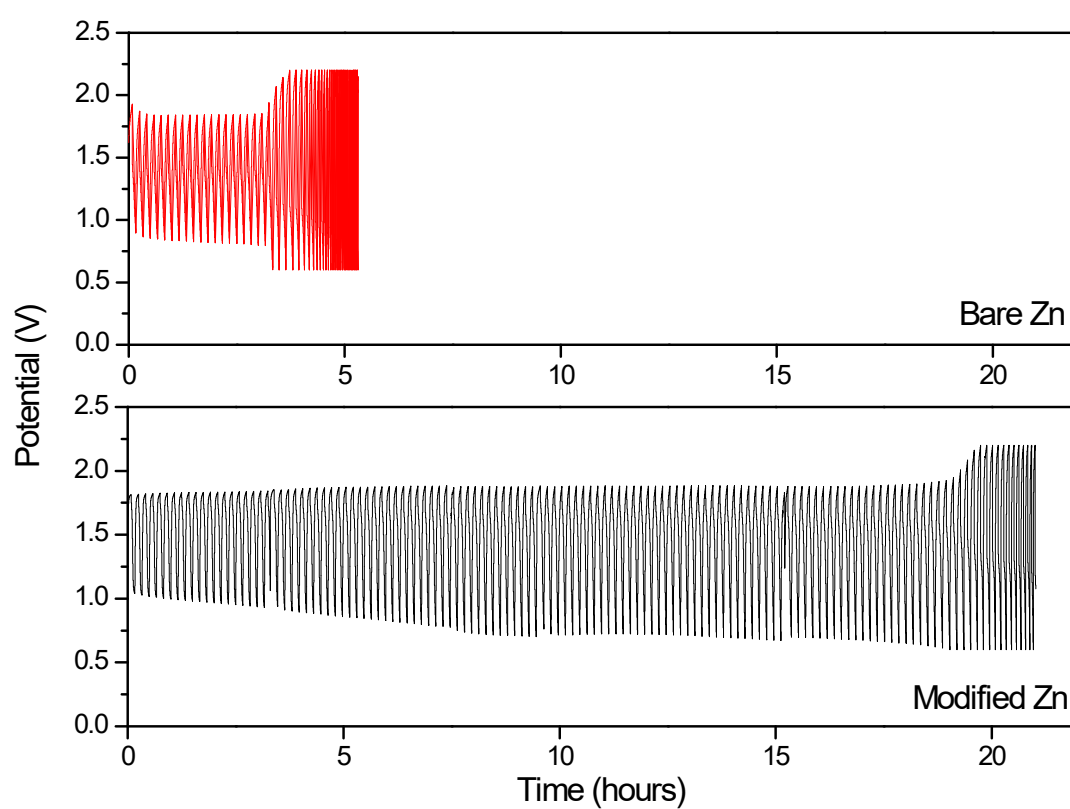
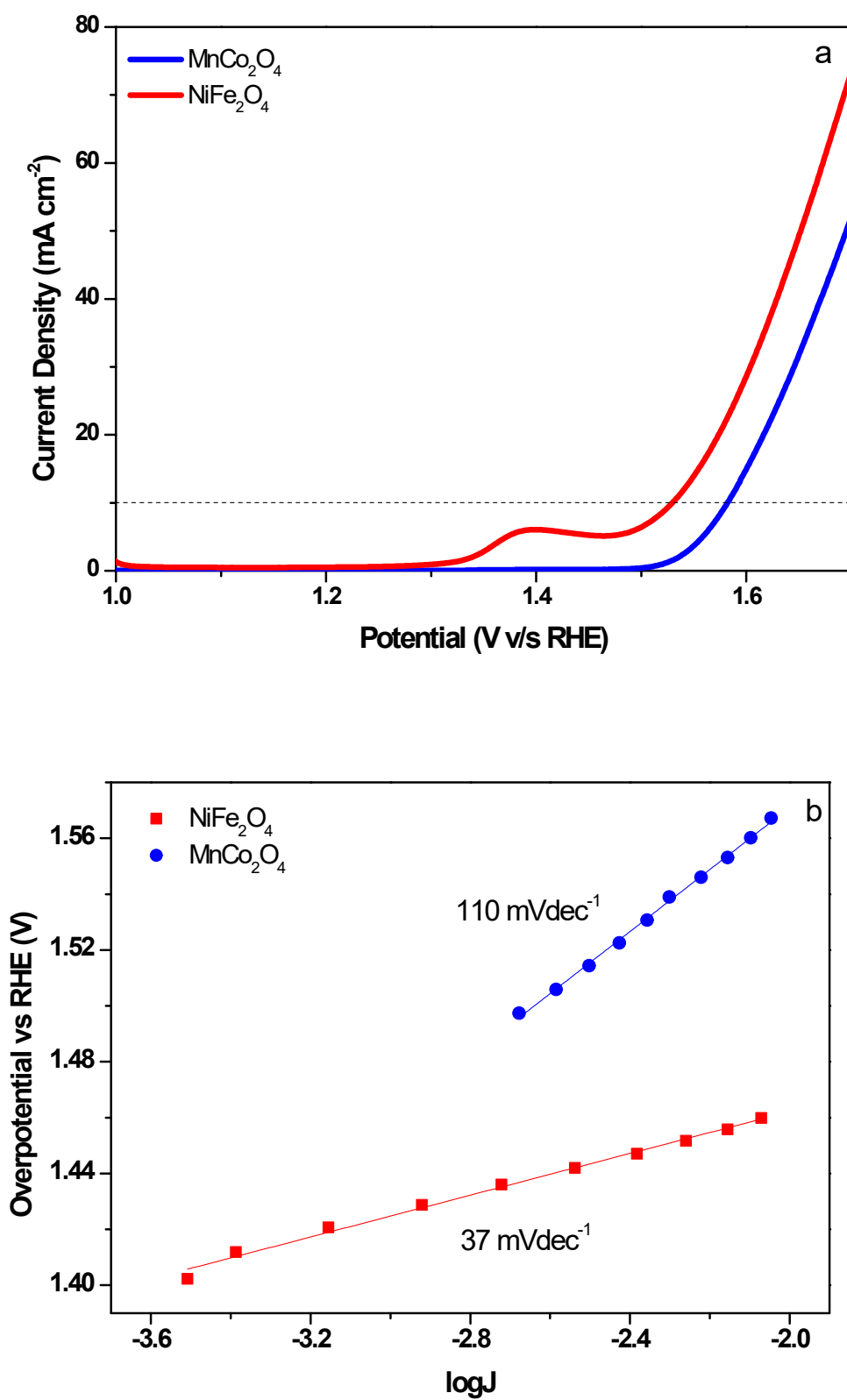


Figure S2: Comparative galvanostatic charge-discharge response of the battery assembled with modified and unmodified anodes with 10 min/ cycle at a current density of 5 mA cm⁻².

Figure S3



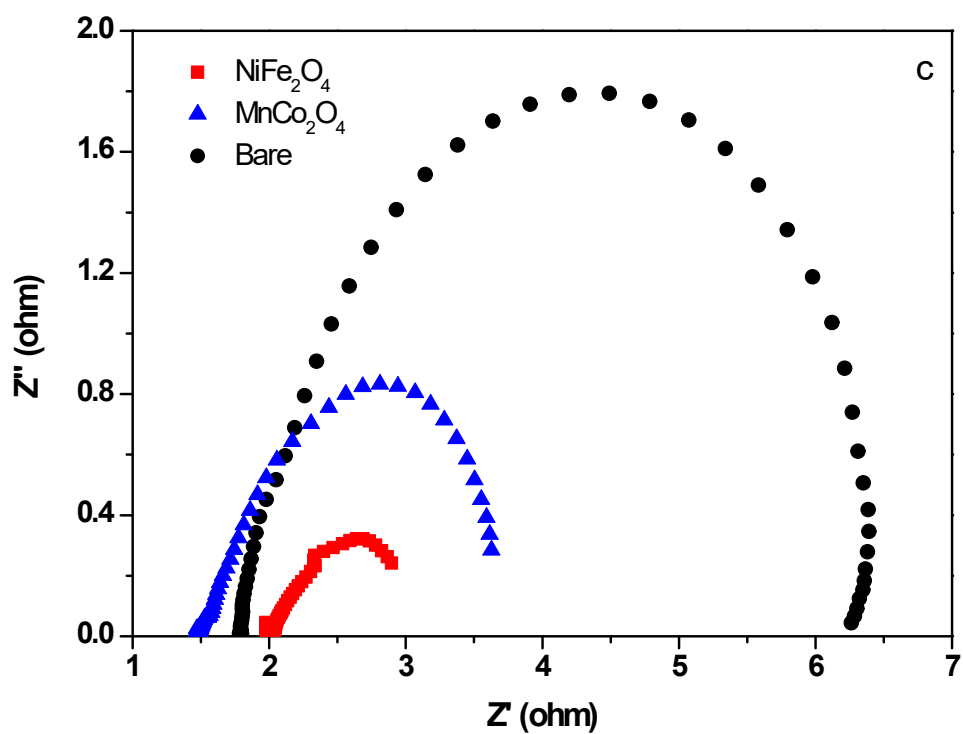


Figure S3: (a) OER polarization curves and (b) the corresponding Tafel plots of NiFe_2O_4 and MnCo_2O_4 catalysts. (c) EIS Nyquist plots and fitting curves at 1.49 V vs. RHE.

Material Stability

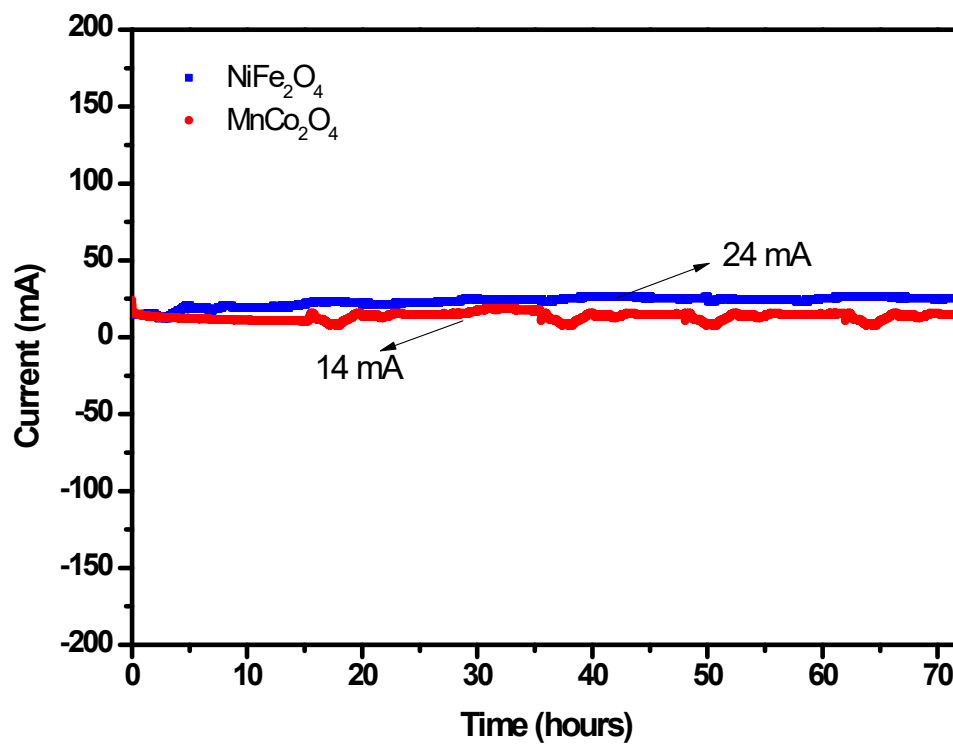
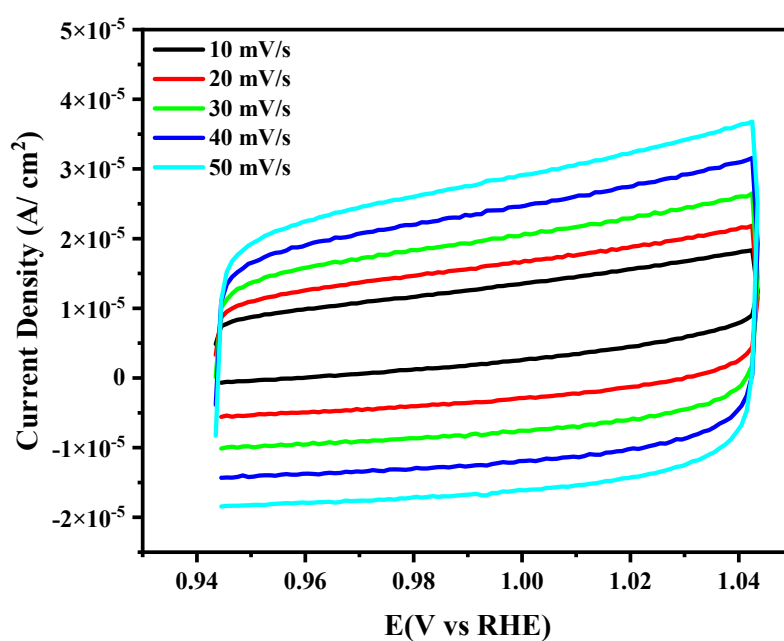


Figure S4: Material stability test of prepared catalysts tested for 72 hours.

Figure S5

The electrochemical surface area (ECSA) is estimated from double-layer electrochemical capacitance (C_{DL}). Figure S5 (a & b) represents the typical CV curves in non-faradaic region at a scan rate ranging from 50 to 150 mV s^{-1} for NiFe_2O_4 and MnCo_2O_4 respectively. At last, the calculated capacitance was further divided by average specific capacitance of $40 \mu\text{F cm}^{-2}$ for the transition metal oxide in 1 M KOH solution to obtain ECSA.



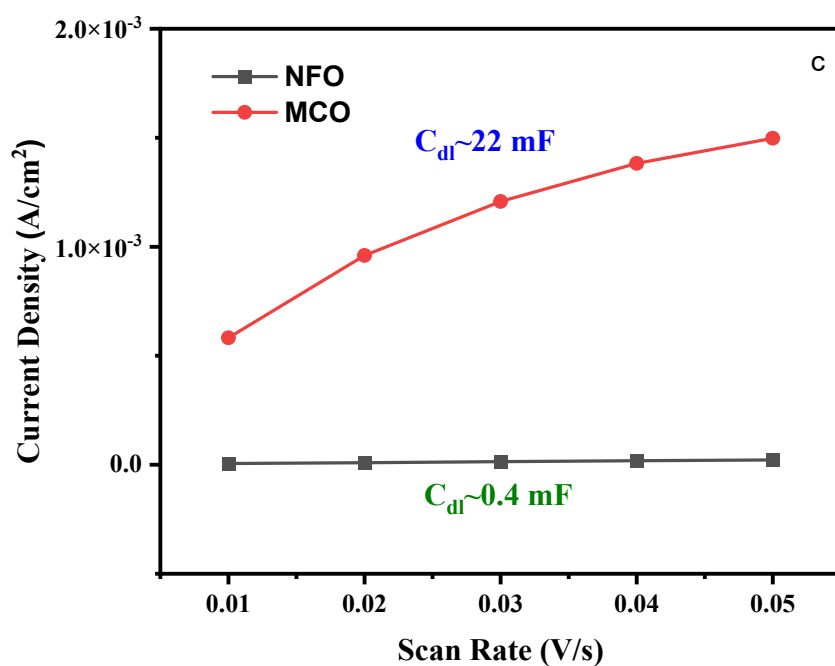
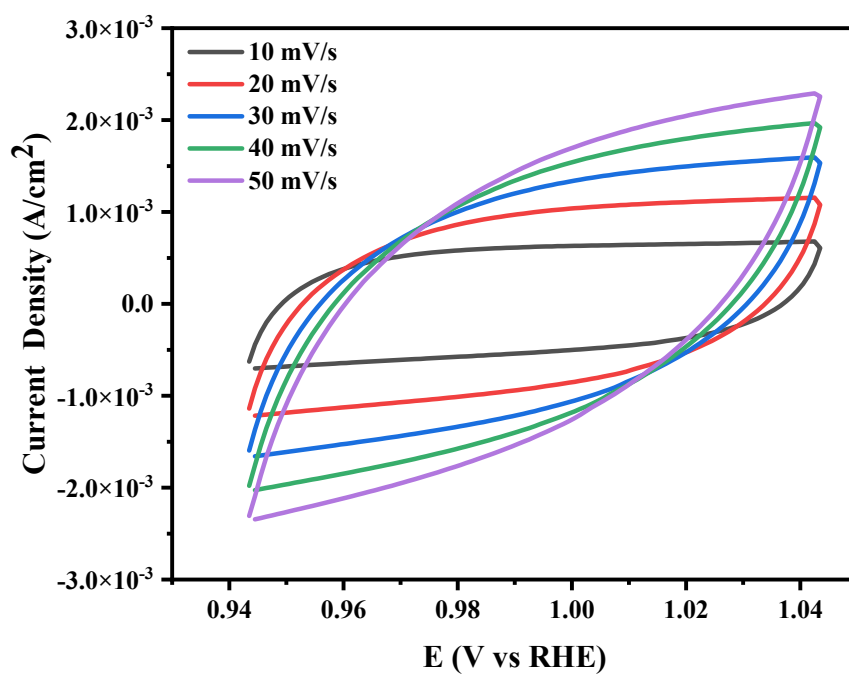
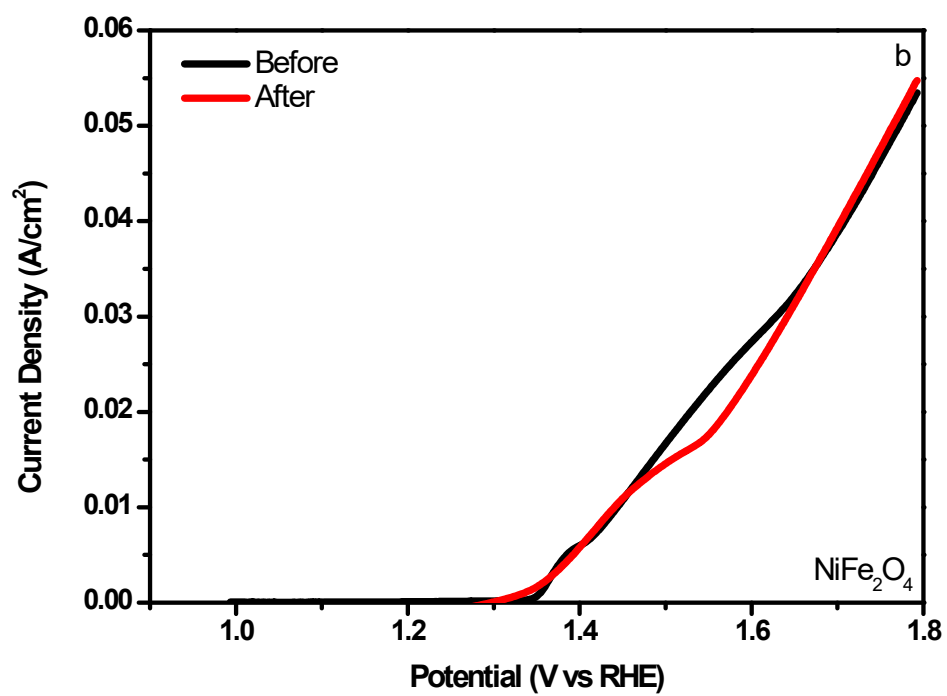
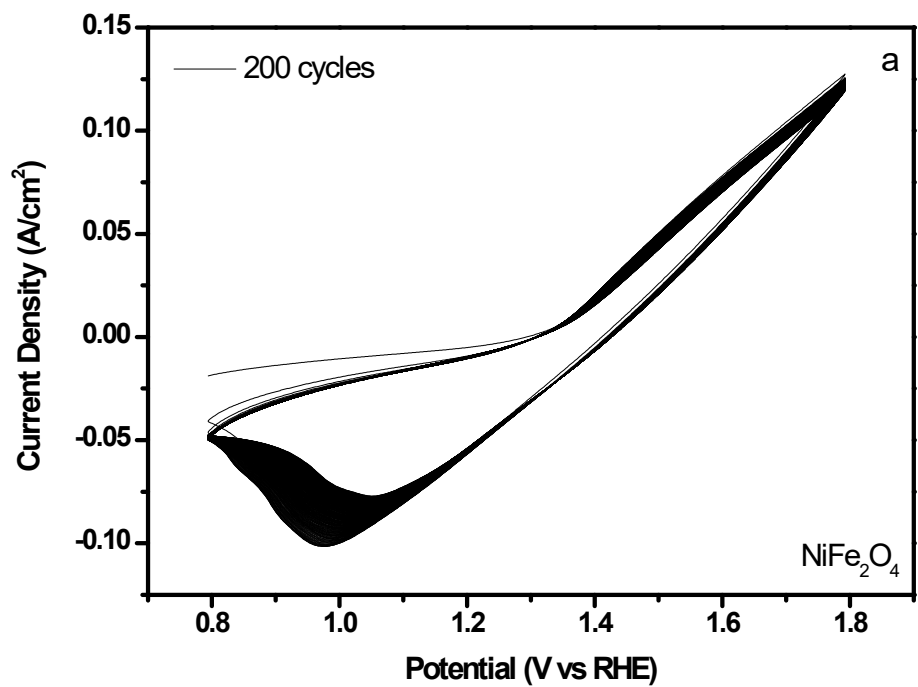


Figure S5: CV curves tested in a non-Faradaic potential range at a scan rate range of 50 to 150 mV s⁻¹ for (a) NiFe₂O₄, (b) MnCo₂O₄, and (c) the calculated double-layer electrochemical capacitance.

Sample	C_{DL} (mF)	ECSA (cm²)
NiFe ₂ O ₄ /NF	0.4	10
MnCo ₂ O ₄ /NF	22	550

Figure S6

Accelerated Data Test (ADT)



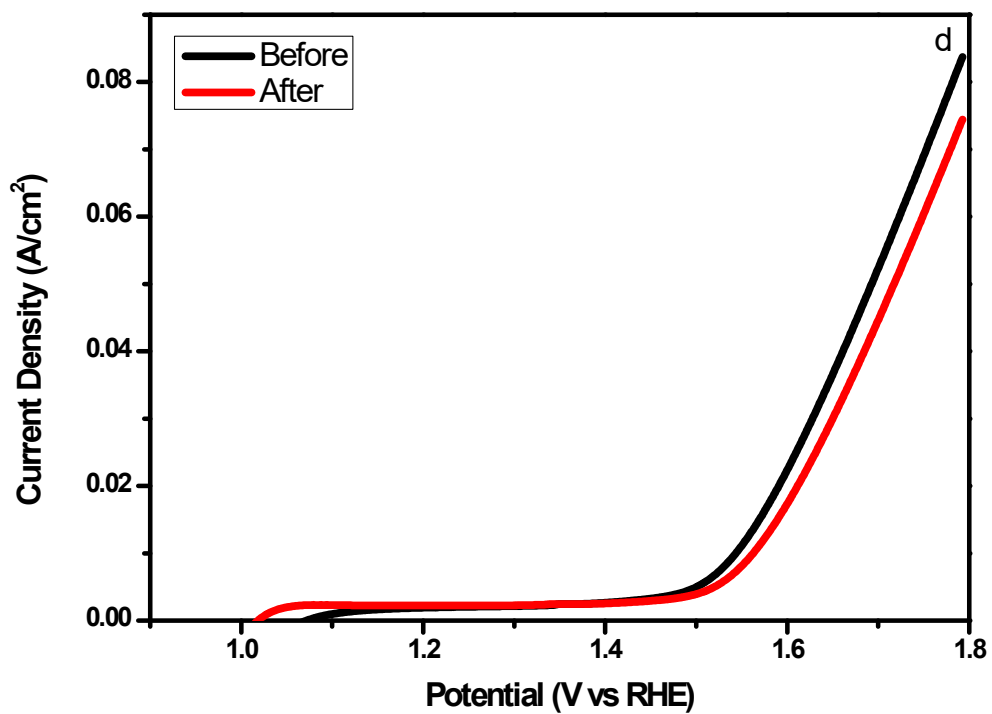
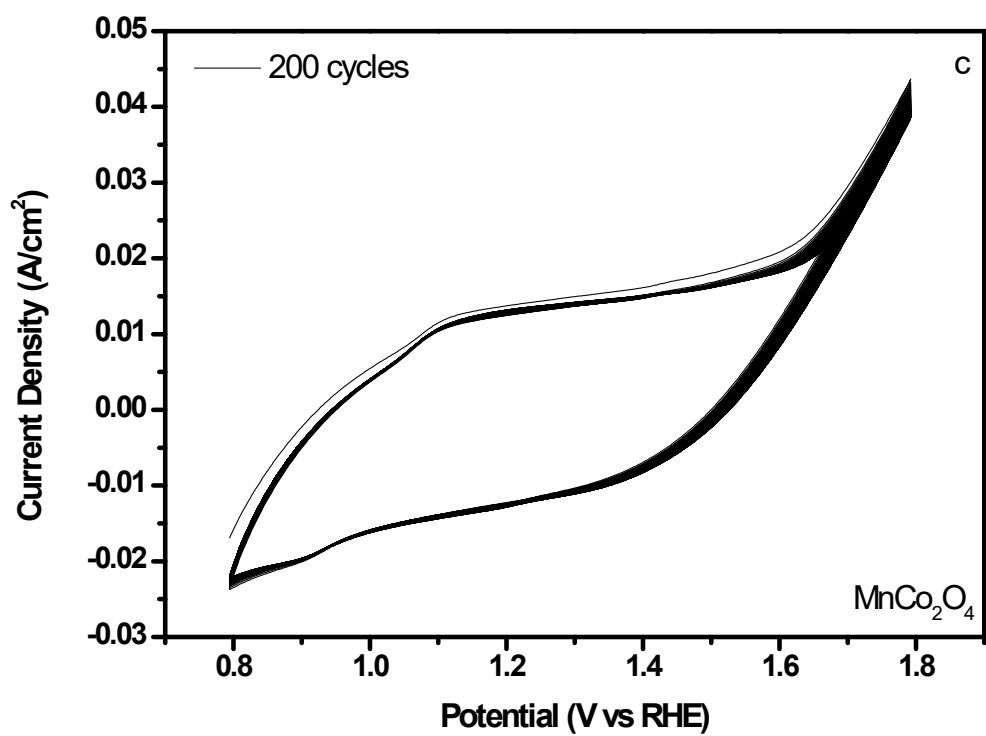


Figure S6: ADT for LSV before and after 200 cyclic voltammetry cycles.